Journal of
Mechanical
Science and
Technology

Journal of Mechanical Science and Technology 21 (2007) 2125~2132

A study on low-velocity impact damage of Z-pin reinforced laminates

Jin Teng[1], Zhuo Zhuang[1,*] and Bintai Li[2]

[1]*School of Aerospace, Tsinghua University, Beijing, 100084*
[2]*Institute of Aeronautical Materials, Beijing, 100095*

(Manuscript Received February 21, 2006; Revised September 7, 2007; Accepted September 18, 2007)

Abstract

Based on a low-velocity impact test, four main modes of low-velocity impact damage, including matrix cracking, delaminating, fiber failure and matrix crushing, are taken into account. By using the proper failure criterion, the low-velocity impact damage of z-pin reinforced laminates can be realized. The results of FEM simulation, which indicate that a z-pin makes the area of delamination reduced by approximately 50%, are in good agreement with the experimental C-scan results.

Keywords: Z-pin reinforcement; Low-velocity impact damage; Delamination; FEM simulation

1. Introduction

Laminates generally have poor through-the-thickness strength. A moderate out-of-plane load can lead to interlaminar delamination and some other modes of damage. To overcome such weakness, the practice of z-pin reinforcement is applied, which involves the direct insertion of reinforcing fibers in the through-the-thickness direction of laminates. The typical z-pin reinforcing process begins with placing a release film, a z-pin preform and a rigid tool onto a laid-up prepreg laminate as shown in Fig. 1 [1]. The z-pin preform consists of structural foam that contains the reinforcing fibers. The laminate is then vacuum bagged and processed by using a standard autoclave cure cycle. During the cure, the heat softens the preform which collapses under the applied pressure. The z-fiber reinforcement is thereby driven into the laminate (the foam is chosen for its ability to provide lateral support to the fibers during the insertion process). On removal from the autoclave, the compacted foam is removed and discarded. The process is completed with the removal of any pin material that projects above the laminate.

*Corresponding author. Tel.: +86 10 62783014
E-mail address: zhuangz@mail.tsinghua.edu.cn

When the matrix is cracked, the fibers can still be intact, and the laminates can continue to sustain additional load [2]. At present, the study of z-pin reinforced laminates is mostly based on steady-state solution. Laminates with 2% volume fraction of the z-pins have been investigated, and the results show that the through-the-thickness Young's modulus is increased by 22-35% with z-pin reinforcement. Compared with the reduction of the in-plane modulus being within 10%, z-pin reinforcement is an economical and efficient process to improve the impact resistance of laminates [3]. The bridging model and the shear-lag model [4] are suggested to investigate the failure mechanisms of fiber-reinforced composites. Based on the shear-lag model, the effect of stress wave has been taken into consideration and the slip, stick and reserve slip characteristics have been analyzed [5].

Most recently, the study of low-velocity impact damage of laminates has mainly been according to numerical simulation based on the low-velocity impact test. The delamination process of composite beams has been analyzed by assuming the penetrated delamination and the critical impact velocity for the delamination growth in the beam model, and using the virtual crack closure technique (VCCT) to calculate the strain energy release rate [6]. A 3D model is

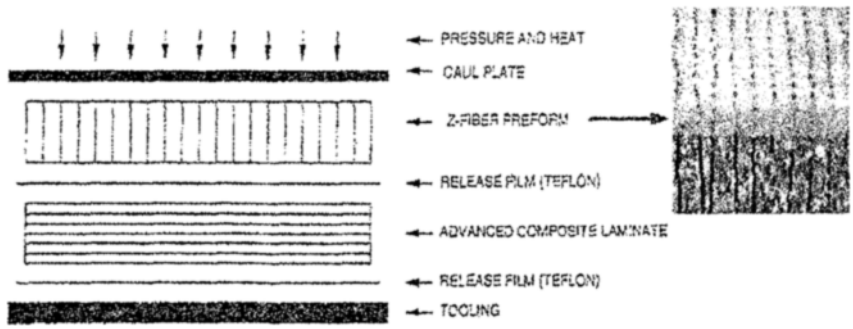

Fig. 1. z-pin reinforcing process.

employed to realize the impact damage by using a failure criterion based on mean stress for matrix cracking and critical stress criterion for delamination [7]. The widely used Chang-Chang failure criterion has been improved to predict the impact damage of laminates [8]. However, the study of low-velocity impact damage of z-pin reinforced laminates has not been reported. This paper develops the 3D finite element model of low-velocity impact damage by associating with z-pin reinforcement mechanism. By using ABAQUS FE code, the low-velocity impact damage of z-pin reinforced laminates can be efficiently simulated by programming user material subroutine VUMAT according to failure criteria and stress update after impact.

2. Failure criteria and stress update

Low-velocity impact damage of composite laminates includes matrix cracking, delamination, fiber failure and matrix crushing. Matrix cracking and delamination are two main modes of impact damage. The failure criteria are formulated below to evaluate fiber failure, matrix cracking and matrix crushing in laminates [8].

2.1 Damage models

Schematics of fiber failure, matrix cracking and matrix crushing models are given in Fig. 2, Fig. 3 and Fig. 4, respectively. The related criteria are also expressed below.

(1) Fiber failure

$$\left(\frac{\sigma_{11}}{X_T}\right)^2+\left(\frac{\sigma_{12}^2+\sigma_{13}^2}{S_f^2}\right)\geq 1 \qquad (1)$$

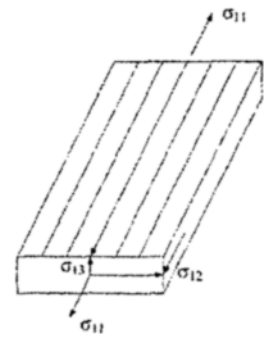

Fig. 2. Schematic of fiber failure.

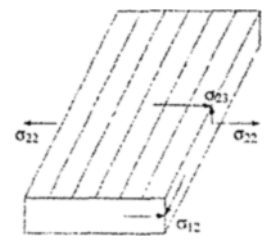

Fig. 3. Schematic of matrix cracking.

(2) Matrix cracking

For $\sigma_{22}\geq 0$,

$$\left(\frac{\sigma_{22}}{Y_T}\right)^2+\left(\frac{\sigma_{12}}{S_{12}}\right)^2+\left(\frac{\sigma_{23}}{S_{m23}}\right)^2\geq 1 \qquad (2)$$

(3) Matrix crushing

For $\sigma_{22}<0$,

$$\frac{1}{4}\left(\frac{-\sigma_{22}}{S_{12}}\right)^2+\frac{Y_c^2\sigma_{22}}{4S_{12}^2Y_c}-\frac{\sigma_{22}}{Y_c}+\left(\frac{\sigma_{12}}{S_{12}}\right)^2\geq 1 \qquad (3)$$

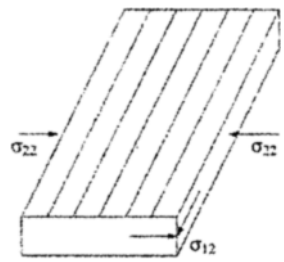

Fig. 4. Schematic of matrix crushing.

Table 1. Damage models and corresponding stress update.

Fiber failure	Matrix cracking	Matrix crushing
D_f=1	D_m=1	D_{mc}=1
$\sigma_{11}=\sigma_{22}=\sigma_{33}=0$ $\sigma_{12}=\sigma_{23}=\sigma_{31}=0$	$\sigma_{22}=0$ $\sigma_{12}=0$	$\sigma_{22}=0$

Where:
X_T-- tensile strength in the fiber direction;
Y_T-- tensile strength in the transverse direction;
Y_C-- compressive strength in the transverse direction;
S_f-- shear strength involving fiber failure;
S_{12}-- shear strength in the fiber and transverse plane;
S_{m23}-- shear strength in the transverse and the through-the-thickness plane.

2.2 Stress update

When stresses of elements satisfy the failure criteria, elements will fail and be unable to transfer load. The post failure behavior is modeled following the damage mechanics. As most graphite/epoxy laminate retains linear elasticity till failure, the corresponding components of stresses will be set to be zero while element fail. The stress update scheme is illustrated in Table 1, where D_f, D_m and D_{mc} stand for damage parameters of fiber failure, matrix cracking and matrix crushing, respectively, with a value of zero or one. A value of zero indicates that the element is active, while a value of one indicates that corresponding stresses should be set to zero. Once the value of damage parameter is set to one, the corresponding stress will remain zero as the actual status.

2.3 Delamination

Delamination is the main mode of low-velocity impact damage of laminates. In order to simulate delamination, the interface is considered as a resin rich zone [9] and a cohesive element in ABAQUS is as

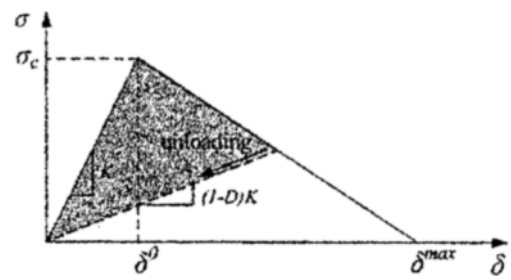

Fig. 5. Bi-linear constitutive equation.

signed to this zone. A linear elastic and linear softening behavior is implemented as shown in Fig. 5 and a high initial stiffness is used to hold the top and bottom faces of the cohesive element together in the linear elastic range. For pure Mode I, II or III loading, after the interfacial normal or shear tractions reach their respective interlaminar tensile or shear strength, the stiffness is gradually reduced to zero [10-12]. The area under the stress-relative displacement curves is the respective (Mode I, II or III) critical strain energy release rate and the equations are given in Eq. (4), where n, s, t represent the normal (I) and the other two shear (II, III) directions, respectively.

$$\begin{aligned}\int_0^{\delta_n^{\max}} t_n(\delta)\,d\delta_n &= G_C^n \\ \int_0^{\delta_s^{\max}} t_s(\delta)\,d\delta_s &= G_C^s \\ \int_0^{\delta_t^{\max}} t_t(\delta)\,d\delta_t &= G_C^t\end{aligned} \tag{4}$$

Therefore, the properties required to define the interfacial behaviors are the initial stiffness, K, the corresponding critical strain energy release rate G_{IC}, G_{IIC}, and G_{IIIC}, and the corresponding interlaminar tensile or shear strength.

A small thickness T_c is assumed for the cohesive zone; the corresponding strains are given by

$$\varepsilon_n=\frac{\delta_n}{T_c},\ \varepsilon_s=\frac{\delta_s}{T_c},\ \varepsilon_t=\frac{\delta_t}{T_c} \tag{5}$$

(1) For $\delta<\delta^0$, the constitutive equation is given by

$$t=\begin{Bmatrix}t_n\\t_s\\t_t\end{Bmatrix}=\begin{bmatrix}K_{nn}&&\\&K_{ss}&\\&&K_{tt}\end{bmatrix}\begin{Bmatrix}\varepsilon_n\\\varepsilon_s\\\varepsilon_t\end{Bmatrix} \tag{6}$$

(2) For $\delta^o \le \delta \le \delta^{max}$, the constitutive equation is given by

$$t = \begin{Bmatrix} t_n \\ t_s \\ t_t \end{Bmatrix} = \begin{bmatrix} (1-D)K_{nn} & & \\ & (1-D)K_{ss} & \\ & & (1-D)K_{tt} \end{bmatrix} \begin{Bmatrix} \varepsilon_n \\ \varepsilon_s \\ \varepsilon_t \end{Bmatrix} \tag{7}$$

Where D is the damage parameter, $0 \le D \le 1$.

(3) For $\delta > \delta^{max}$, all the penalty stiffness reverts to zero and interlaminar delamination occurs.

In structural application of laminates, delamination growth is more likely to occur under mix-mode loading. The B-K criterion [10] is particularly useful when the critical fracture energies during deformation purely along the first and the second shear directions are the same, i.e., $G_s^C = G_t^C$. It is given by

$$G^C = G_n^C + \left(G_s^C - G_n^C\right)\left(\frac{G_S}{G_T}\right)^{\eta} \tag{8}$$

where $G_S = G_s + G_t$, $G_T = G_n + G_S$, η is a material parameter, for glass/epoxy laminates, $\eta = 2 \sim 3$; for graphite/epoxy laminates, $\eta = 1 \sim 2$ [13]. When G_n^C, G_s^C and η are defined, the critical strain energy release rate G^C is a definition function of G_S / G_T.

3. Experimental work

The impact test of z-pin reinforced laminates was accomplished by the Beijing Institute of Aeronautical Materials. The experimental T300/3234 z-pin reinforced laminate specimen is shown in Fig. 6 and the material properties are given as the following:

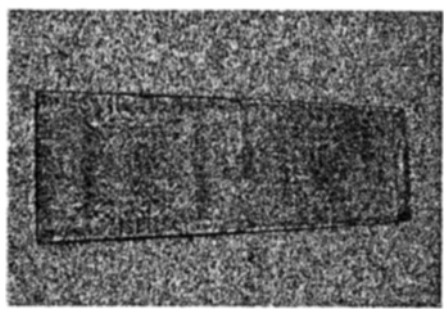

Fig. 6. Z-pin reinforced laminate specimen.

(1) Epoxy resin:
ρ: 1.2g /cm^3
Elongation percentage: 2.8%
Tensile strength: 73MPa
Tensile modulus: 3.3GPa
Shear strength: generally between 25MPa and 35MPa

(2) T300-6000-50B fiber:
ρ: 1.81g/cm^3
Elongation percentage: 1.5%
Tensile strength: 3500MPa
Tensile modulus: 230GPa

(3) T300/3234 laminate:
Volume fraction of fiber: 63±3%
ρ: 1.55-1.60g /cm^3
Tensile strength in 0° direction: 1530MPa
Tensile modulus in 0° direction: 128GPa
Compressive strength in 90° direction : 1060MPa
υ_{12} : 0.32
Tensile strength in 90° direction: 60MPa
Tensile modulus in 90° direction: 8.3GPa
Shear modulus in 1-2 plane: 5GPa
Interlaminar shear strength: 86MPa

(4) Properties of interface:
$G_{IC} = 151\ J/m^2$, $G_{IIC} = 500\ J/m^2$, $\eta = 1.55$

The schematic of drop-weight test is shown in Fig. 7. The impact energy can be calculated with 4.45J per millimeter; thus the impactor height can be obtained. The specimen lay-up consisting of 32 plies is $[45°/0°/-45°/90°]_{4s}$ with each ply thickness 0.125mm. The experimental parameters are given as the following:

Specimen size: 150mm ×100mm
Aperture size: 125mm ×75mm
z-pin diameter: 1.12mm
z-pin spacing: 1cm square pitch arrangement
Impactor diameter: 12.5 mm
Impactor weight: 5kg

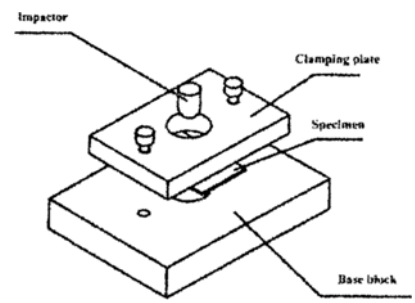

Fig. 7. Schematic of drop-weight test.

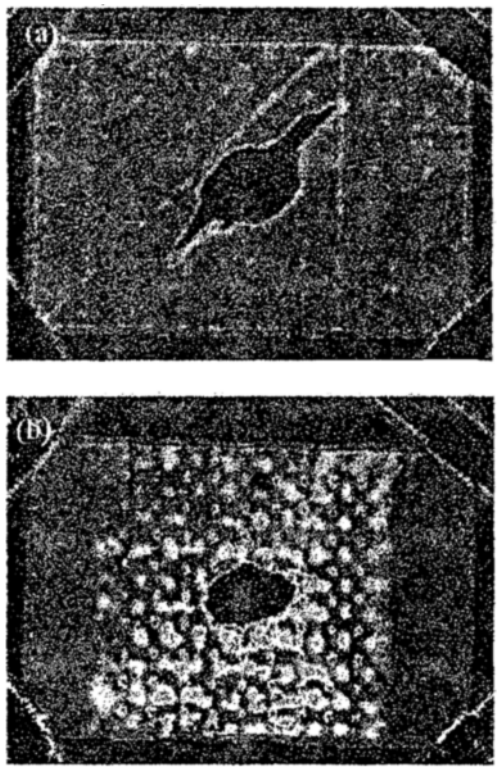

Fig. 8. C-scan maps of delamination after impact.

The C-scan results after impact are shown in Fig. 8, and the center areas in black represent the delamination areas. The delamination area of laminates without z-pin reinforcement is shown in Fig. 8a, for which the area is 9.8 cm^2, the length is 3.3cm in 0° direction, 2.7cm in 90° direction and 7.2cm in 45° direction, respectively. The delamination area with z-pin reinforcement is shown in Fig. 8b, for which the area is 4.9 cm^2, and the length is 3.1cm in 0° direction, 2.2cm in 90° direction, respectively. Hence, z-pin reinforcement makes the delaminating area reduced by 50%.

4. Numerical simulation

The impact test model as shown in Fig. 6 can be divided into four parts: impactor, ply of laminates, interlaminar cohesive zone and z-pins. The impactor is considered as a rigid ball with a punch diameter. The ply of laminates is quasi-isotropic. A cohesive element is assigned to the interlaminar cohesive zone. And laminates are simply supported. Two low-velocity impact tests with different epoxy laminates are implemented to verify the rationale of this FE model.

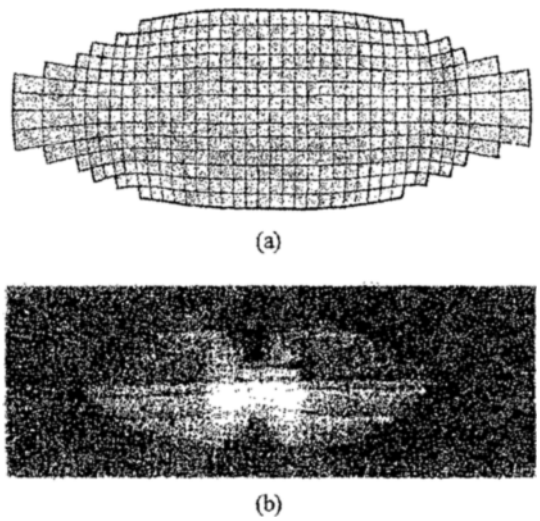

Fig. 9. Delamination area of glass/epoxy laminates.

4.1 Comparison examples

4.1.1 Glass/epoxy laminates

Experimental data of glass/epoxy laminates are presented as the following [7]:

(1) Rigid ball: m=2.3kg, v=4.85m/s

(2) $[0_4/90_2/0_4]$, ply thickness is 1.8×10^{-4}m, circular simply supported with diameter is 0.16m, $\rho=$ 1678kg/m^3

(3) $E_1=30.5$GPa, E_2=E_3=6.9GPa, $\upsilon_{12}=\upsilon_{13}=0.344$, $\upsilon_{23}=0.46$, G_{23}=1.6GPa, G_{12}=G_{13}=4.65GPa

(4) X_T=700MPa, Y_T=100MPa, Y_C=237MPa, S_{12}=64MPa, S_{m23}=200MPa, S_t=120MPa

(5) Properties of interface

$G_{IC}=120\ J/m^2$, $G_{IIC}=1200\ J/m^2$, $\eta=2.6$

As shown in Fig. 9(a), the delaminating length from FE simulation is 7.8cm in 0° direction, 2.6cm in 90° direction, respectively, and the area is 16cm^2. Compared with this is the experimental data given in Fig. 9b, for which the length is 8.2cm in 0° direction and 2.7cm in 90° direction, respectively, and the area is 16.8cm^2. Although the experimental result seems even more like a butterfly shape, the two results are very close to each other. Within consideration of the dispersibility of the experiment test, the FE results correspondence matches the experimental data.

4.1.2 Graphite/epoxy laminates

Experimental data of graphite/epoxy laminates are presented as the following [8]:

(1) Rigid ball: m=0.26kg, v=7.08m/s

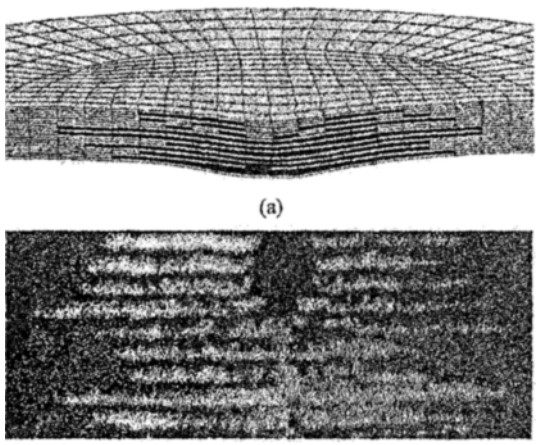

Fig. 10. Delamination of graphite/epoxy laminates.

(2) [0/90] alternate, 21 plies with total thickness is 2.6×10^{-3}m, circular simply supported with diameter is 0.045m, $\rho=1583$kg/m^3

(3) $E_1=139$Gpa, E_2=E_3=9.4Gpa, $\upsilon_{12}=\upsilon_{13}=0.309$, $\upsilon_{23}=0.33$, G_{23}=2.98Gpa, G_{12}=G_{13}=4.5Gpa

(4) X_T=2070Mpa, Y_T=74Mpa, Y_C=237Mpa, S_{12}=64 Mpa, S_{m23}=64Mpa, S_f=120Mpa

(5) Properties of interface
$G_{IC}=240\ J/m^2$, $G_{IIC}=750\ J/m^2$, $\eta=1.55$

Delamination of graphite/epoxy through the thickness is shown in Fig. 10. The maximum length of delaminating from the FE result shown in Fig. 10a is about 20mm, which is in good agreement with the experimental one shown in Fig. 10b with a value of about 19mm.

Through the two examples above, the FE model can efficiently and correctly simulate the delamination of epoxy laminates with different kinds of fibers. By improving this FE model, low-velocity impact damage of z-pin reinforced laminates can be realized.

4.2 Simulation for z-pin reinforced laminates

The application of z-pins is to preclude the interlaminar delamination. Therefore, only the z-pins around the impact point are considered, other z-pins are omitted. Z-pins are not fractured after impact tests, so the relative displacements of z-pins and laminates are also omitted. The resin between z-pins and laminates is replaced by a tie constraint in the FE model. Fig. 11a is an illustration of an FE model of laminates without z-pin reinforcement and Fig. 11b is the FE model with z-pin reinforced laminates.

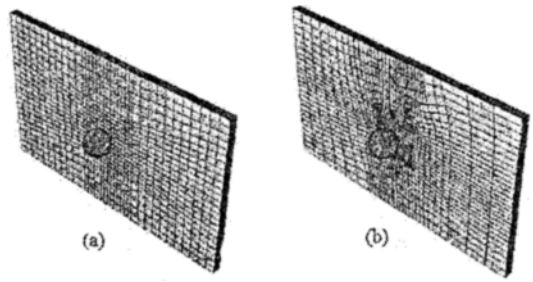

Fig. 11. FE model for low-velocity impact of laminates.

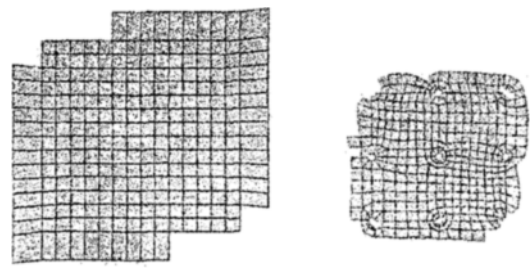

Fig. 12. The predicted delamination area of laminates.

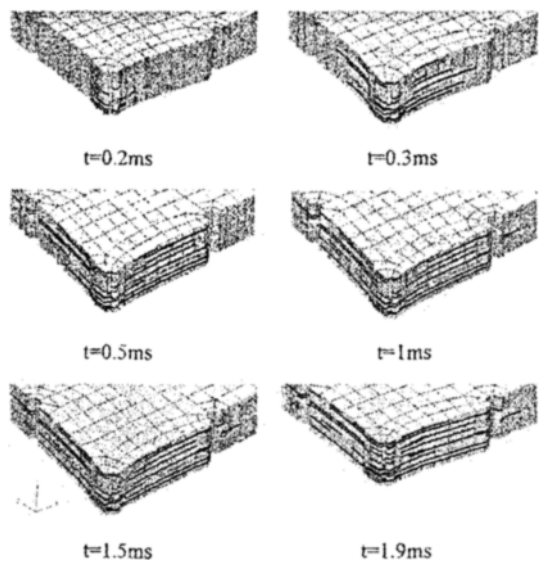

Fig. 13. Predicted delamination from FE model.

(1) Low-velocity impact damage

The predicted delamination area of laminates without z-pin reinforcement is shown in Fig. 12a, for which the area is 11.7cm^2 and the length is 3.8cm in 0° direction, 3.4cm in 90° direction and 5.6cm in 45° direction, respectively. The predicted delaminating area with z-pin reinforced laminates is shown in Fig.

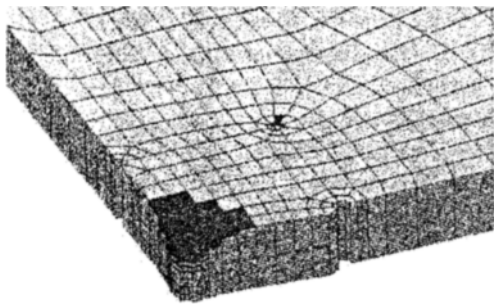

Fig. 14. Predicted matrix crushing from FE model.

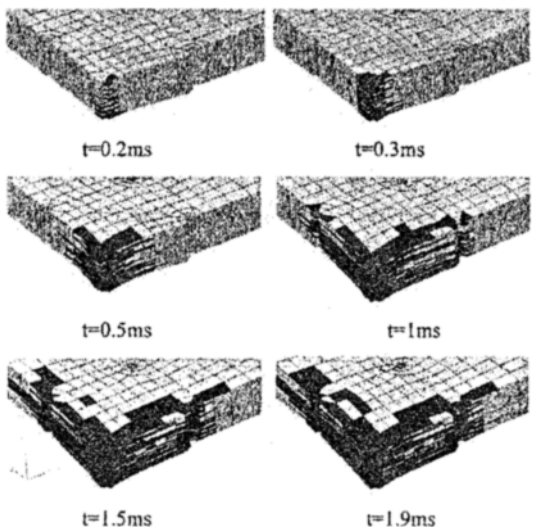

Fig. 15. Predicted matrix cracking from FE model.

12b, for which the area is 5.8cm^2 and the length is 2.6cm in 0° direction, 2.6cm in 90° direction, respectively. Due to the interaction between z-pins and laminates, the predicted delamination area is reduced by 50.6%. Furthermore, delamination at each characteristic time is illustrated in Fig. 13.

Besides delamination, matrix cracking and matrix crushing can also appear in the laminates. Because the impact energy of this experiment is not large enough, fiber failure is rarely found and could be not taken into discussion. Predicted matrix cracking is presented in Fig. 14 and predicted matrix crushing at each characteristic time is illustrated in Fig. 15.

(2) Impact response

The curve of impact load–displacement of an impactor before failure occurs in the laminates is displayed in Fig. 16. The spring stiffness of z-pin reinforced laminates is 4.5×10^6 N/m, which is 21.6%

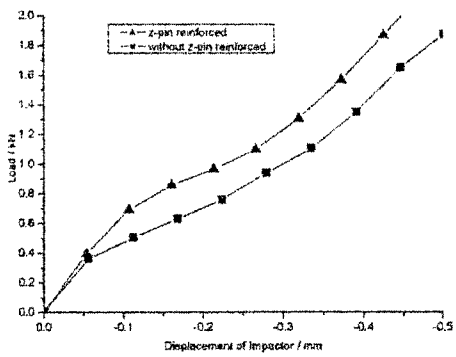

Fig. 16. Load-displacement curve of impactor.

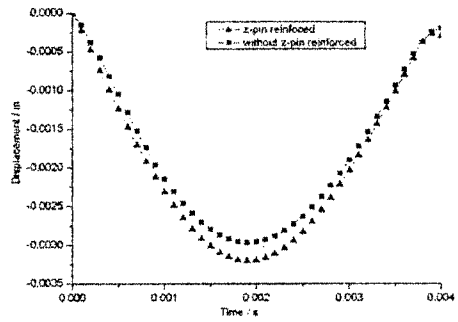

Fig. 17. Deflection of central point in the mid-plane of laminates.

higher than that of laminates without z-pin reinforcing with the value 3.7×10^6 N/m.

It is shown in Fig. 17 that the maximum deflection of the central point in the mid-plane of z-pin reinforced laminates is greater than that of laminates without z-pin reinforcing. Hence, a z-pin makes a little bit of a reduction of the in-plane stiffness demonstrated.

The kinetic energy of the model could be divided into two parts: one is assigned to the impactor and the other is assigned to laminates, and the latter one's occupation rate is very small. A comparison of the two models' kinetic energy variation during impacting is illustrated in Fig. 18. The initial kinetic energy of both models is 17.8J; while for impact completed, the kinetic energy of the model without z-pin reinforcement is 11J. The reason for the reduction is the dissipation of energy due to damage and the conversion into strain energy of laminates which will finally dissipate according to the damping action. As a result of less damage in laminates, the kinetic energy of the model with z-pin reinforced is 12.3J while impact completed is 1.3J larger than that of model without z-pin reinforced.

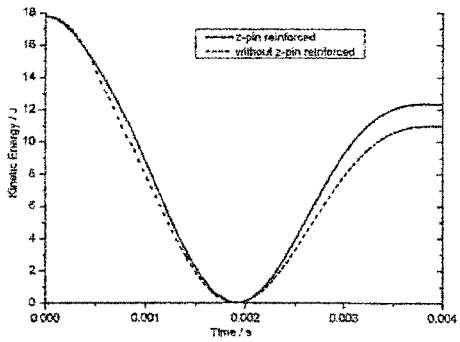

Fig. 18. Kinetic energy of model.

5. Conclusion

Four modes of low-velocity impact damage of laminates, including fiber failure, matrix cracking, matrix crushing and delamination have been realized by implementation of improving failure criteria and application of COHESIVE ELEMENT. The prediction of low-velocity impact damage of laminates has been achieved with 1% volume fraction of z-pins, which is 1.12mm diameter for each z-pin. The conclusions are given below:

(1) The reduction of delamination area is 50.6% through the FEM simulation, which is in good agreement with the experimental C-scan data 50%.

(2) Z-pin reinforcement makes an increment of 21.6% of through-the-thickness stiffness, but little reduction of in-plane stiffness.

(3) After impact, the kinetic energy of the model will decrease due to damage dissipation and there is less damage in laminates owing to z-pin reinforcement.

Considering computational cost, only z-pins around the impact point have been taken into account and the variation of material orientation of areas around the z-pins due to the insertion of z-pins is also omitted in this FE model. Moreover, additional stress concentration around z-pins can also affect the enlargement of FE results. All of these shortages will be improved in further work.

Reference

[1] D. J. Barrett, The mechanics of z-fiber reinforcement, Composite Structures, 36 (1996) 23-32

[2] Y. C. Gao, Damage modeling of fiber reinforced composites, *Theo. Appl. Frac. Mech.* 11 (3) (1989) 147-155.

[3] M. Grassi, X. Zhang, M. Meo, Prediction of stiffness and stresses in z-fiber reinforced composite laminates, *Composites: Part A.* 33 (2002) 1653-1664.

[4] Y. C. Gao, Y. W. Mai, B. Cotterell, Fracture of fibre reinforced material, *J. Appl. Math. Phys.* 39 (1988) 550-572.

[5] N. Sridhar, Q. D. Yang, B. N. Cox, Slip, stick, and reverse slip characteristics during dynamic fiber pullout, *Journal of the Mechanics and Physics of Solids.* 51 (2003) 1215-1241.

[6] C. T. Sun, J. E. Grady, Dynamic delamination fracture toughness of a Graphite/epoxy laminate under impact, *J. Composite Science and Technology.* 31 (1988) 55-72.

[7] F. Collombet, X. Lalbin and J. L. Lataillade, Impact behavior of laminated composites: physical basis for finite element analysis, *Composites Science and Technology.* 58 (1998) 463-478.

[8] J. P. Hou, N. Petrinic, C. Ruiz and S. R. Hallett, Prediction of impact damage in composite plates, *Composite Science and Technology.* 60 (2000) 273-281.

[9] L. Daudeville, O. Allix, and P. Ladevèze, Delamination Analysis by Damage Mechanics: Some Applications, Composites Engineering, 5(1) (1995): 17-24.

[10]ABAQUS Analysis User's Manual, v6.5, ABAQUS INC., USA, (2005).

[11]P. P. Camanho, C. G. Dávila and D. R. Ambur, Numerical Simulation of Delamination Growth in Composite Materials, NASA/TP-2001-211041.

[12]C. G. Dávila and P. P. Camanho, Analysis of the effects of residual strains and defects on skin/stiffener debonding using decohesion elements, NASA-AIAA-2003-1465.

[13]M. L. Benzeggagh and M. Kenane, Measurement of Mixed-Mode Delamination Fracture Toughness of Unidirectional Glass/Epoxy Composites with Mixed-Mode Bending Apparatus, *Composites Science and Technology.* 56 (1996) 439–449.